

2-Piperidino-1,1,2-triphenylethanol: A Highly Effective Catalyst for the Enantioselective Arylation of Aldehydes

Montserrat Fontes, Xavier Verdaguer, Lluís Solà, Miquel A. Pericàs,* and Antoni Riera

Unitat de Recerca en Síntesi Asimètrica (URSA-PCB), Parc Científic de Barcelona and Departament de Química Orgànica, Universitat de Barcelona, Josep Samitier 1-5, E-08028 Barcelona, Spain

mapericas@pcb.ub.es

Received December 16, 2003

Here we report the use of 2-piperidino-1,1,2-triphenylethanol (**5**) as an outstanding catalyst for the ligand-catalyzed arylation of aldehydes. The use of **5** and a 2/1 mixture of Et₂Zn/Ph₂Zn provided the corresponding chiral diarylcarbinols with enantiomeric excess of up to 99% ee. The effect of temperature on the reaction enantioselectivity was studied and the inversion temperature (*T*_{inv}) was determined to be 10 °C for reaction with *p*-tolylaldehyde. Most remarkably, lowering the amount of catalyst (**5**) to 0.5 mol % still afforded excellent levels of enantiocontrol (93.7% ee). Kinetics of the catalyzed and uncatalyzed arylation of aldehydes was studied by means of in situ FT-IR. The background uncatalyzed addition rates to *p*-tolylaldehyde when using pure Ph₂Zn and Et₂Zn/Ph₂Zn (2/1) suggest that in the latter case a mixed zinc species forms (EtPhZn) minimizing the undesired nonselective addition. Formation of EtPhZn was modeled at the DFT calculation level. A four-center TS (**TS-V**) corresponding to the Et/Ph scrambling was localized along with two dimers (**D-IV** and **D-VI**). The model supports the hypothesis that Et/Ph exchange is a kinetically facile process. Gas evolution experiments during the formation of the active catalyst showed that the formation of an active site with a ONZn-Et (**10**) moiety is kinetically favored over ONZn-Ph (**11**). Finally, the phenyl transfer to benzaldehyde was modeled at the PM3(tm) level through anti and syn 5/4/4 tricyclic TS structures for both **10** and **11**. The model could correctly predict the sense and selectivity of the overall process and predicted that **11** should be more selective than **10**.

Introduction

Enantiomerically pure diarylmethanols are the basis of economically and therapeutically important medicines such as (*R*)-neobenodine, (*R*)-orphenadrine, or (*S*)-carbinoxamine.¹ Besides the reduction of appropriate diaryl ketones, where the achievement of high enantioselectivities can become problematic when the two aryl groups are similar in volume or electronic nature, the enantioselective arylation of aldehyde substrates appears to be the most promising alternative for the preparation of these molecular systems.² However, the development of an enantioselective Ph₂Zn addition to aldehydes is a challenging endeavor compared to the related and well-studied diethylzinc addition. The main difficulty that hampers the asymmetric aryl transfer is the background-uncatalyzed addition that competes with the ligand-catalyzed reaction. Diarylzinc species are several orders of magnitude more reactive toward aldehydes than the corresponding alkyl species (Et₂Zn, Me₂Zn, Prⁱ₂Zn), and such an enhanced reactivity gives rise to the undesired direct addition of Ar₂Zn to the carbonyl compound

providing racemic product arylcarbinol that lowers the overall system performance.³

Starting from the pioneering work of Fu, who reported in 1997 the addition of salt-free Ph₂Zn to *p*-chlorobenzaldehyde using a planar-chiral azaferrocene ligand with moderate enantioselectivity,⁴ much effort has been dedicated to the generation of a practical system for the highly enantioselective arylation of aromatic aldehydes. Since then, two major approaches have been devised to minimize the competing uncatalyzed process. On one hand, Pu and co-workers found that carrying out the addition reaction at low concentrations improved dramatically the enantioselectivity when using a chiral binaphthol ligand **1**.⁵ Alternatively, Bolm and co-workers have developed an effective reagent system that involves the use of a Ph₂Zn/Et₂Zn mixture to suppress the

(1) (a) Harms, A. F.; Nauta, W. T. *J. Med. Pharm. Chem.* **1960**, *2*, 57–77. (b) Sperber, N.; Papa, D.; Schwenk, E.; Sherlock, M. *J. Am. Chem. Soc.* **1949**, *71*, 887–890.

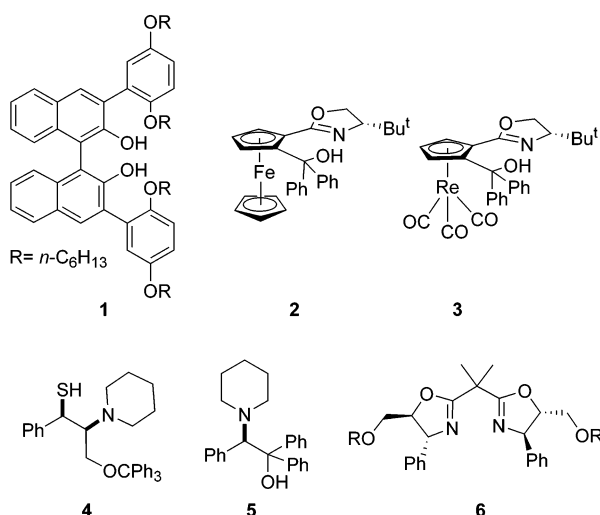
(2) For asymmetric hydrogenation and oxazaborolidine reduction of benzophenones see: (a) Ohkuma, T.; Koizumi, M.; Ikehira, H.; Yokozawa, T.; Noyori, R. *Org. Lett.* **2000**, *2*, 659–662. (b) Corey, E. J.; Helal, C. J. *Tetrahedron Lett.* **1996**, *37*, 5675–5678. (c) Corey, E. J.; Helal, C. J. *Tetrahedron Lett.* **1995**, *36*, 9153–9156.

(3) (a) Bolm, C.; Hildebrand, J. P.; Muniz, K.; Hermanns, N. *Angew. Chem., Int. Ed.* **2001**, *40*, 3284–3308. For leading references on aryl transfer to ketones see: (b) Ramón, D. J.; Yus, M. *Tetrahedron* **1998**, *54*, 5651–5666. (c) Ramón, D. J.; Yus, M. *Eur. J. Org. Chem.* **2003**, 2745–2748. (d) Jeon, J.-S.; Walsh, P. J. *J. Am. Chem. Soc.* **2003**, *125*, 9544–9545. (e) Dosa, P. I.; Fu, G. C. *J. Am. Chem. Soc.* **1998**, *120*, 445–446. For general reviews on enantioselective addition of organozincs to aldehydes see: (f) Soai, K.; Niwa, S. *Chem. Rev.* **1992**, *92*, 833–856. (g) Pu, L.; Yu, H.-B. *Chem. Rev.* **2001**, *101*, 757–824. (h) Noyori, R.; Kitamura, M. *Angew. Chem., Int. Ed. Engl.* **1991**, *30*, 34–48.

(4) Dosa, P. I.; Ruble, J. C.; Fu, G. C. *J. Org. Chem.* **1997**, *62*, 444–445.

(5) (a) Huang, W.-S.; Hu, Q.-S.; Pu, L. *J. Org. Chem.* **1999**, *64*, 7940–7956. (b) Huang, W.-S.; Pu, L. *J. Org. Chem.* **1999**, *64*, 4222–4223.

undesired background reaction.⁶ Employing ferrocenyl oxazoline **2** and rhenium-tricarbonyl oxazoline **3** ligands a highly enantioselective aryl transfer was achieved for a variety of arylaldehydes. The same catalytic system also has been applied to the phenyl transfer to *N*-formyl-imines.⁷ Whereas the Bolm methodology allows the addition reactions to be performed at synthetically useful concentrations within reasonable reaction times, the achievement of high enantioselectivities relies on rather complex ligands and requires their use in substantial amounts. In contrast, Ha and co-workers, reported recently that when using a biaryl derived amino-alcohol the combination of Ph_2Zn and Et_2Zn provides a decreased isolated yield of product carbinol.⁷ Despite these advances, a practical solution for the highly enantioselective arylation of aldehydes involving the use of a readily available ligand and low catalyst loading has still to be developed.



In the past few years we have reported the synthesis of new families of β -amino alcohol (**5**),⁸ β -amino thiol (**4**),⁹ and bis(oxazoline) (**6**)¹⁰ ligands ultimately arising from the regioselective and stereospecific ring opening of epoxides obtained by Sharpless and Jacobsen epoxidations. The main advantages of these ligands are the broad variety of structural types they can cover and their

(6) (a) Bolm, C.; Hermanns, N.; Hildebrand, J. P.; Muniz, K. *Angew. Chem., Int. Ed.* **2000**, *39*, 3465–3467. (b) Bolm, C.; Kesselgruber, M.; Hermanns, N.; Hildebrand, J. P.; Raabe, G. *Angew. Chem., Int. Ed.* **2001**, *40*, 1488–1490. (c) Bolm, C.; Muniz, K. *Chem. Commun.* **1999**, 1295–1296. (d) Hermanns, N.; Dahmen, S.; Bolm, C.; Brase, S. *Angew. Chem., Int. Ed.* **2002**, *41*, 3692–3694. For the enantioselective aryl transfer from $\text{Ar}(\text{OH})_2/\text{Et}_2\text{Zn}$ see: (e) Bolm, C.; Rudolph, J. *J. Am. Chem. Soc.* **2002**, *124*, 14850–14851.

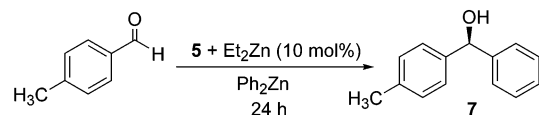
(7) Ko, D.-H.; Kim, K. H.; Ha, D.-C. *Org. Lett.* **2002**, *4*, 3759–3762.

(8) (a) Vidal-Ferran, A.; Moyano, A.; Pericàs, M. A.; Riera, A. *J. Org. Chem.* **1997**, *62*, 4970–4982. (b) Vidal-Ferran, A.; Bampos, N.; Moyano, A.; Pericàs, M. A.; Riera, A.; Sanders, J. K. M. *J. Org. Chem.* **1998**, *63*, 6309–6318. (c) Jimeno, C.; Pasto, M.; Riera, A.; Pericàs, M. A. *J. Org. Chem.* **2003**, *68*, 3130–3138. (d) Solà, L.; Reddy, K. S.; Vidal-Ferran, A.; Moyano, A.; Pericàs, M. A.; Riera, A.; Alvarez-Larena, A.; Piniella, J. F. *J. Org. Chem.* **1998**, *63*, 7078–7082. (e) Reddy, K. S.; Solà, L.; Moyano, A.; Pericàs, M. A.; Riera, A. *J. Org. Chem.* **1999**, *64*, 3969–3974. (f) Reddy, K. S.; Solà, L.; Moyano, A.; Pericàs, M. A.; Riera, A. *Synthesis* **2000**, *2000*, 165–176.

(9) Jimeno, C.; Moyano, A.; Pericàs, M. A.; Riera, A. *Synlett* **2001**, 1155–1157.

(10) Pericàs, M. A.; Puigjaner, C.; Riera, A.; Vidal-Ferran, A.; Gomez, M.; Jimenez, F.; Müller, G.; Rocamora, M. *Chem. Eur. J.* **2002**, *8*, 4164–4178.

TABLE 1. Phenyl Transfer Reactions at Room Temperature (aldehyde concentration 10 mM)



entry	solvent	yield (%)	ee (%) ^a
1	hexane	57	73
2	toluene	29	50
3	THF	2	10
4	Et_2O	29	78
5 ^b	Et_2O		48
6	CH_2Cl_2	16	13

^a Enantiomeric excess was determined by HPLC analysis of the corresponding carbinol. ^b Reaction performed with no Et_2Zn .

modular construction, which allows the easy modification of their structures at any step of the synthesis. These characteristics have been shown to be of fundamental importance for the fine-tuning of catalytic activity and enantioselectivity, and have allowed the ex novo design of optimal ligands for a variety of important reactions.

Among these ligands, 2-piperidino-1,1,2-triphenylethanol (**5**),^{8d,11} available on the mol scale in both enantiomeric forms through two simple operations from commercially available triphenylethylene, occupies a singular position. Not only does it exhibit a very high catalytic activity in the ethylation of aldehydes of all structural types, but it also shows a very high enantioselectivity at low catalyst loading in these additions provided that the carbon α to the formyl group bears at least two carbon substituents.

The characteristics of 2-piperidino-1,1,2-triphenylethanol discussed above rendered this amino alcohol a promising candidate ligand for the enantioselective arylation of benzaldehydes. In particular, both the preferential recognition of one of the enantiotopic faces of the substrate and a good level of suppression of the background reaction through its high catalytic activity were anticipated. We wish to report in this paper how these initial ideas have been elaborated and have led to the establishment of 2-piperidino-1,1,2-triphenylethanol (**5**) as a most practical ligand for the enantioselective aryl transfer of Ph_2Zn to aldehydes.

Results and Discussion

Phenyl Transfer under High Dilution Conditions.

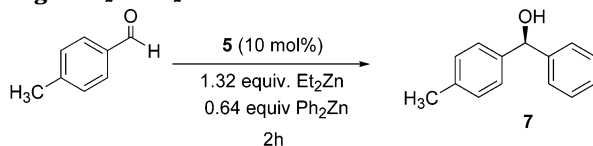
Pu and co-workers used the binol-derived catalyst **1** pretreated with 2.0 equiv of diethylzinc.^{5a} The authors assume that the zinc complex generated from the reaction of **1** with diethylzinc is a better catalyst than the one generated with Ph_2Zn . In addition, the right choice of solvent for each substrate and the use of additives (MeOH) proved to be critical to obtain high enantioselectivity. We first investigated the addition of Ph_2Zn to *p*-tolylaldehyde under high dilution conditions (10 mM) using 10 mol % of 2-piperidino-1,1,2-triphenylethanol (**5**) pretreated with an equimolar amount of Et_2Zn . The results when performing the reaction in different solvents are displayed in Table 1. The best enantioselectivities

(11) 2-Piperidino-1,1,2-triphenylethanol (**5**) is commercially available in both enantiomeric forms.

SCHEME 1



TABLE 2. Asymmetric Phenyl Transfer Reactions Using a Ph₂Zn/Et₂Zn Mixture^a



entry	solvent	T (°C)	yield (%)	ee (%) ^b
1	toluene	rt	98	96
2	toluene	0	85	97
3	hexane	rt	94	97
4	hexane	0	90	98
5	Et ₂ O	0	80	96
6 ^c	toluene	rt	90	88

^a Aldehyde concentrations approximately 100 mM. ^b Enantiomeric excess was determined by HPLC analysis of the corresponding carbinol. ^c 1.2 equiv of Ph₂Zn was used and no extra Et₂Zn was added.

(78% ee) could be observed when using diethyl ether as solvent (entry 4). Hexane gave rise to slightly lower selectivity but with higher conversion numbers (entry 1). As reported, not pretreating the ligand with Et₂Zn had a deleterious effect and the enantiomeric excess of the resulting carbinol (**7**) dropped to 48% ee (entry 5). Throughout the study utilizing high dilution conditions the yields and conversion numbers were not satisfactory and in most experiments starting material remained unconsumed after extended reaction time (24 h) even at room temperature.

Phenyl Transfer Using a Ph₂Zn/Et₂Zn Mixture.

The use of mixed zinc species in asymmetric catalysis is a well-documented strategy when a valuable alkyl radical is to be completely transferred.¹² Knochel and co-workers developed the bis[(trimethylsilyl)methyl]zinc **8** which, in the presence of a diorganozinc compound (R₂Zn), leads to the formation of R-Zn-CH₂Si(CH₃)₃ (**9**).¹³ In the newly formed organometallic complex the (trimethylsilyl)methyl group acts as a nontransferable group in the ligand-catalyzed addition to aldehydes. NMR experiments support the existence of mixed (β-silylalkyl)-Zn-alkyl species in equilibrium with the starting symmetric zinc compounds.¹³ Although no real evidence exists for the related Ph₂Zn/Et₂Zn mixture, a similar equilibrium has been postulated for the formation of the mixed EtPhZn complex.^{6a} Under these circumstances only the phenyl group on Zn is transferred and the ethyl group would act as a nontransferable radical.

We explored the use of an excess of Et₂Zn (1.32 equiv) along with 0.64 equiv of Ph₂Zn with *p*-tolylaldehyde as a test substrate (Table 2). From the very beginning the effectiveness of ligand **5** for the asymmetric phenyl transfer in combination with the mixed zinc species was

evident. The addition reaction in toluene at room temperature afforded the corresponding carbinol **7** in 96% ee and 98% isolated yield (Table 2, entry 1). Decreasing the reaction temperature to 0 °C had a slightly positive effect on selectivity and provided **7** in 97% ee (Table 2, entry 2). Hexane was a somewhat better solvent for this process giving rise to the product with 97% and 98% ee at room temperature and 0 °C, respectively (Table 2, entries 3 and 4). Except for in diethyl ether, addition reactions went to completion within 2 h even at 0 °C. Concentration did not seem to be a critical issue with this protocol. All reactions in Table 2 were performed at an aldehyde concentration of 100 mM. However, an aldehyde concentration of 250 mM in hexane afforded the product alcohol in an excellent 95% ee. Under the present set of conditions, the aryl transfer was completely selective over the ethylation process and no ethyl addition product could be detected in the final reaction mixtures. Finally, to check whether the excess of Et₂Zn was of any benefit, a blank experiment lacking the additive was carried out (Table 2, entry 6). Without diethylzinc an extremely fast reaction took place and the product was obtained in high yield but decreased optical purity (88% ee). This confirmed the use of Ph₂Zn/Et₂Zn mixtures as a clear advantage when using **5** as a catalyst.

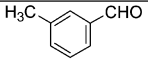
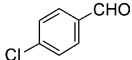
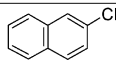
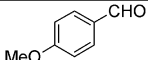
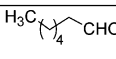
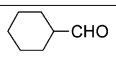
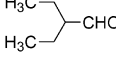
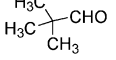
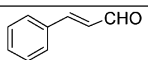
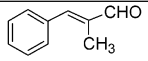
With the purpose of determining the scope and utility of the present system (Ph₂Zn/Et₂Zn and **5**) for the asymmetric arylation of aldehydes a series of substrates with diverse steric and electronic properties was investigated (Table 3). It should be emphasized that the level of enantiocontrol for all aromatic substrates is outstanding. The corresponding diarylcarbinols are obtained in optical purities in the range of 93% to 98% enantiomeric excess. Hexane was used as the solvent of choice. Most intriguingly, similar enantioselectivities were achieved working either at 0 °C or room temperature (vide infra). This could conveniently simplify the experimental procedure and represents an important improvement with respect to previously reported catalytic systems. Ortho-substituted benzaldehydes are good substrates and lead to excellent enantiomeric excess (Table 3, entries 1, 4, and 5). On the other hand, linear aliphatic aldehydes provide poorer selectivities. Addition to *n*-heptanal yielded the product alcohol in 63% ee (Table 3, entry 9). Increasing the steric bulk of the carbon chain resulted in higher enantioselectivities (Table 3, entries 10–12). Finally, a significant solvent dependence was observed for α,β-unsaturated aldehydes (Table 3, entries 13 and 14). In the case of (*E*)-α-methylcinnamaldehyde, running the reaction in toluene instead of hexane confers a jump in enantiomeric excess from 87% to 94%. An assessment of the data exposed in Table 3 shows that, since outstanding results were obtained for aromatic and fully substituted aliphatic aldehydes (Table 3, entries 12 and 14), it is necessary to have no hydrogens α to the carbonyl to obtain high enantioselectivity. This is in contrast with the geometric requirements found for the ethylation process when using **5** as a catalyst where a single substituent α to the aldehyde is sufficient to reach high ee. For example, cyclohexylcarbaldehyde provides 98% ee in the Et₂Zn addition compared to 60% ee (Table 3, entry 10) in the arylation reaction.^{8d}

Comparison of the absolute configuration of the product alcohols in Table 3 with the stereochemistry of β-amino

(12) (a) Wipf, P.; Ribe, S. *J. Org. Chem.* **1998**, *63*, 6454–6455. (b) Lalöe, E.; Srebnik, M. *Tetrahedron Lett.* **1994**, *35*, 5587–5590. (c) Lutz, C.; Knochel, P. *J. Org. Chem.* **1997**, *62*, 7895–7898. (d) Traverse, J. F.; Hoveyda, A. H.; Snapper, M. L. *Org. Lett.* **2003**, *5*, 3273–3275.

(13) Berger, S.; Langer, F.; Lutz, C.; Knochel, P.; Mobley, T. A.; Reddy, C. K. *Angew. Chem., Int. Ed. Engl.* **1997**, *36*, 1496–1498.

TABLE 3. Arylation Reaction with Different Aldehydes^a

Entry	R-CHO	Solvent	T (°C)	Yield	ee (%) ^b	Config.
1		hexane	0	99	96	S
2		hexane	0	84	98	S
3		hexane	r.t.	82	95	S
4		hexane	0	91	93	S
5		hexane	0	61	98	S
6		hexane	r.t.	70	96	S
7		hexane	r.t.	91	95	S
8		hexane	0	r.t.	97	S
9		hexane	0	84	63	R
10		hexane	0	96	60	R
11		hexane	0	80	83	R
12		hexane	r.t.	85	92	R
		hexane	0	91	97	
13		hexane	0	78	79	R
		toluene	0	84	82	
14		hexane	0	95	87	R
		toluene	0	98	94	

^a Reactions were carried out in the presence of 10 mol % of **5** using a mixture of 0.64 equiv of Ph₂Zn and 1.32 equiv of Et₂Zn.
^b Enantiomeric excess was determined by chiral HPLC analysis.

alcohol **5** enabled us to ascertain that the present arylation process follows the empirical rule that Noyori established for the ethylation process.¹⁴ (*R*)-Piperidino-1,1,2-triphenylethanol exclusively catalyzed the phenyl addition to the *Si* face of the starting aldehyde.

Interested by the uncommon behavior we encountered in this system in terms of selectivity and reaction temperature (*vide supra*), we decided to examine it more closely. We soon discovered that the temperature dependence became more perceptible when reducing the amount

of catalyst in the reaction mixture. Thus, the relationship between enantiomeric excess and temperature was investigated at 1 mol % catalyst loading, between 0 and 25 °C, for the Ph₂Zn/Et₂Zn addition to *p*-tolylaldehyde (Figure 1). In both toluene and hexane a maximum enantioselectivity was observed when the reaction was performed around 10 °C. From that point, either raising or lowering the temperature has a deleterious effect on reaction selectivity. Such behavior can be rationalized according to the isoinversion principle.¹⁵ When a chemical

(14) Noyori, R.; Kitamura, M. *Angew. Chem., Int. Ed. Engl.* **1991**, *30*, 49–69.

(15) Buschmann, H.; Scharf, H.-D.; Hoffmann, N.; Esser, P. *Angew. Chem., Int. Ed. Engl.* **1991**, *30*, 477–515.

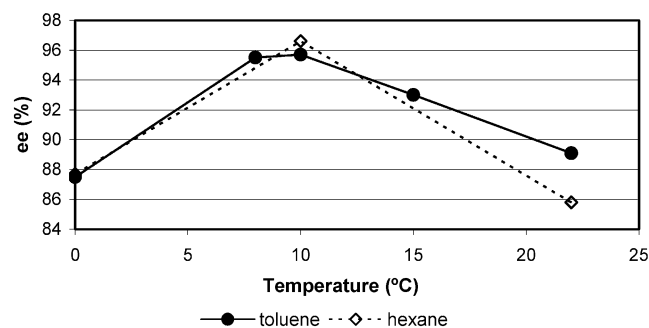


FIGURE 1. Enantioselectivity vs temperature in the arylation of *p*-tolylaldehyde (**5**, 1 mol %).

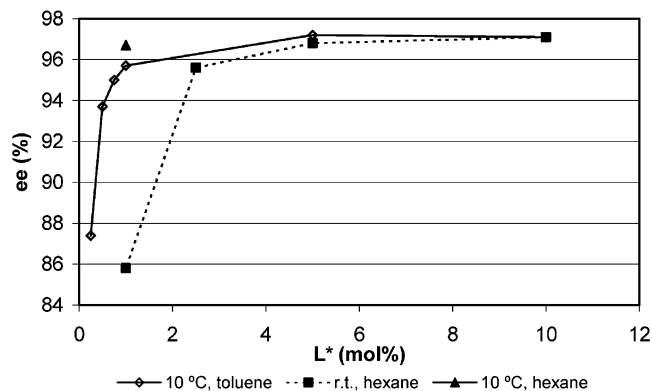


FIGURE 2. Enantioselectivity vs catalyst loading in the arylation of 4-methylbenzaldehyde.

process shows for a selectivity property (enantio-, regio-, or chemoselectivity) two distinct linear regions in the Eyring graph, the temperature at which the inversion occurs is called the inversion temperature (T_{inv}). In our system and for the case of *p*-tolylaldehyde T_{inv} is approximately 10 °C. Other examples of similar temperature dependence in asymmetric catalysis can be found in the oxazaborolidine-mediated borane reduction of prochiral ketones¹⁶ or in the thoroughly studied transition-metal-catalyzed hydrogenation.¹⁷ To know the inversion temperature for the system at hand is of tremendous importance in terms of process optimization. In our case, performing the reaction at 10 °C allowed the catalyst loading to be reduced to 1 mol % with practically no loss of enantioselectivity (96.6% ee).

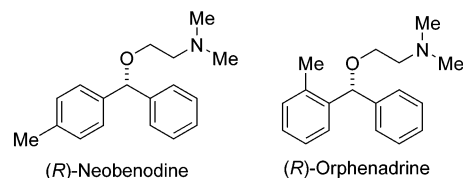
At hand there was a tremendously active catalytic system, since with 1 mol % of **5**, reactions were complete within 2–3 h. This discovery encouraged us to further investigate the limits of the arylation reaction in terms of catalyst loading. The enantiomeric excess observed versus the amount of catalyst is depicted in Figure 2. We were pleased to find that working at the inversion temperature (10 °C) and a catalyst loading of 0.5 mol % still afforded excellent levels of enantiocontrol (93.7% ee). Hexane was once again slightly more efficient a solvent than toluene in the phenyl addition to *p*-tolylaldehyde. At 1 mol % of catalyst loading (10 °C) the product alcohol

TABLE 4. Arylation Reactions at 10 °C Using 1.5 mol % of **5**^a

Entry	R-CHO	Yield (%)	ee (%) ^a
1		90	95
2		86	99
3		85	94
4		94	91
5		79	95
6		65	92

^a Enantiomeric excess was determined by chiral HPLC analysis.

was obtained in enantiomeric excess one point higher (96.7% ee) than that observed in toluene. Running the reaction in hexane at room temperature, a higher temperature than T_{inv} , was shown to be less effective, although the more practical procedure with regard to reaction conditions may pay off a slight decrease on enantioselectivity. To exemplify the effectiveness of the present catalytic system even at low catalyst loadings a series of substrates were submitted to the phenyl addition using 1.5 mol % of **5** at 10 °C (Table 4). Excellent yields and enantioselectivities were obtained for a wide range of aromatic aldehydes. Most remarkably, to our knowledge the highest ever observed enantiomeric excess in Ph_2Zn addition to aldehydes (99% ee) was attained for 4-phenylbenzaldehyde (Table 4, entry 2). In addition, diarylcarbinols derived from asymmetric phenyl addition to *p*-tolylaldehyde and *o*-tolylaldehyde (Table 4, entries 1 and 3) can be valuable intermediates in the asymmetric synthesis of antihistaminic neobenodine and orphenadrine drugs.¹



In Situ FT-IR Study of the Arylation Process.

Despite the efficiency of the present catalytic system, little is known about the factors which make it so effective. In the reaction mixture there are several zinc species: Ph_2Zn , Et_2Zn , and the postulated PhEtZn , which could, in principle, add to the starting aldehyde. A working hypothesis is that diphenyl- and diethylzinc are in equilibrium with phenyldiethylzinc and that the new mixed alkylarylzinc, being less reactive than Ph_2Zn , helps to suppress the background uncatalyzed arylation reaction. However, there is no experimental evidence sup-

(16) (a) Puigjaner, C.; Vidal Ferran, A.; Moyano, A.; Pericàs, M. A.; Riera, A. *J. Org. Chem.* **1999**, *64*, 7902–7911. (b) Corey, E. J.; Bakshi, R. K.; Shibata, S. *J. Am. Chem. Soc.* **1987**, *109*, 5551–5553.

(17) (a) Ojima, I.; Kogure, T.; Yoda, N. *J. Org. Chem.* **1980**, *45*, 4728–4735. (b) Sinou, D. *Tetrahedron Lett.* **1981**, *22*, 2987–2998.

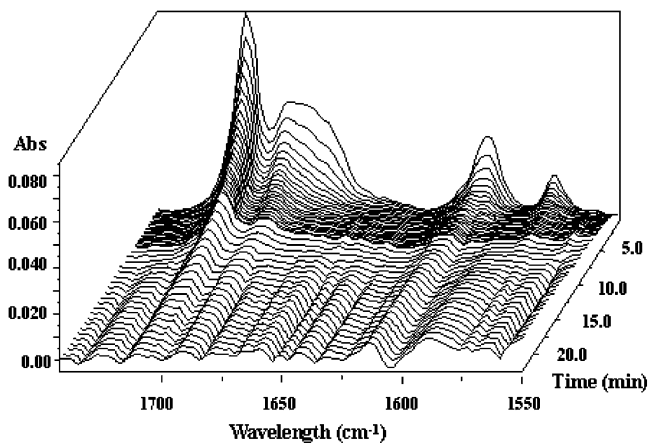


FIGURE 3. In situ FT-IR spectra of the reaction mixture.

porting this hypothesis.¹⁸ To shed light onto these questions we undertook a study of the arylation process by means of in situ FT-IR technology.¹⁹ FT-IR allowed the disappearance of the starting aldehyde to be monitored through its C=O absorbance at different time intervals. IR spectra were recorded with a ReactIR 1000 fitted with an immersible DiComp ATR probe. A representative reaction spectrum series for the arylation of *p*-tolylaldehyde is shown in Figure 3.

We first focused on the rate evaluation of the catalyzed versus the uncatalyzed addition reaction to *p*-tolylaldehyde (0.25 M) using either pure Ph₂Zn or the Ph₂Zn/Et₂Zn (1/2) mixture. Reactions were carried out in toluene at 0 °C employing the standard reaction conditions. The corresponding plots of absorbance versus time are shown in Figure 4. With Ph₂Zn (0.27 M) alone the uncatalyzed arylation reaction is surprisingly rapid at 0 °C and the reaction went to completion within approximately 25 min. The presence of 2.5 mol % of **5** with Ph₂Zn (0.27 M) accelerated the addition reaction to the point that it reached completion in 5 min. On the other hand, when the Ph₂Zn/Et₂Zn (0.16 and 0.33 M) mixture was employed the direct background addition was extremely slow at 0 °C, almost negligible, while the **5** (2.5 mol %) catalyzed arylation proceeded fast enough to be over within 15 min. Despite the rate enhancement observed when using **5** as a catalyst, the background reaction when using pure Ph₂Zn is fast enough to successfully compete with the catalyzed process and cause a decrease in selectivity as can be observed in the product enantioselectivity (Table 2, Entry 6). In contrast, when using the Et₂Zn/Ph₂Zn mixture the catalyzed arylation is slightly slower than that with pure Ph₂Zn, but the rate difference with the background reaction is greatly increased.

The uncatalyzed addition rates were next investigated at different reaction temperatures to fully describe the

background reaction when using pure Ph₂Zn and the Ph₂Zn/Et₂Zn (2/1) mixtures. The corresponding plots are depicted in Figures 5 and 6. In the case of the mixed zinc reagent (Figure 6) the recorded reaction rates were extremely slow even at 30 °C. The half-life of the starting aldehyde at 10 °C was estimated to be 5.7 h.²⁰ From data in Figure 6, initial rate constants k_v^0 were calculated by adjusting the aldehyde absorbance (concentration) to a second-order rate law expression as has been proposed for the addition of Grignard reagents to ketones.^{21,22} Linear least-squares fitting of calculated k_i against $1/T$ permitted the estimation of activation energy (E_a) at 70.1 kJ·mol⁻¹ (16.7 kcal·mol⁻¹) for the background Ph₂Zn/Et₂Zn addition process. In a similar fashion from data in Figure 5, the half-life for the direct addition of pure Ph₂Zn at 10 °C was 6.0 min and the E_a was evaluated to be 13.8 kJ·mol⁻¹ (3.3 kcal·mol⁻¹).²³ This value is lower than that found for the addition of 2-methoxyphenylmagnesium bromide to di-*tert*-butyl-ketone in THF (41.5 kJ·mol⁻¹),²⁴ but is in the same range as the E_a found for the reaction of heptylmagnesium bromide with CO₂ (17.6 kJ·mol⁻¹).^{25,26} These data support the hypothesis that when mixing diphenylzinc and diethylzinc (1:2), Ph₂Zn is depleted from the reaction medium and that a new kind of zinc complex forms that barely reacts with the aldehyde in the absence of the catalyst, thus minimizing the background reaction.

DFT Computational Study on the Formation of the Mixed Zinc Species. Diorganozinc compounds that contain saturated alkyl groups always occur as monomers in solution.^{27,28} The zinc in these compounds is unable to attain coordination saturation through the formation of alkyl bridges, as occurs in the lower dialkylmagnesium compounds. Bridging alkyl groups between zinc and zinc centers have only been postulated as transition species in the exchange of alkyl groups.²⁸ On the other hand, alkynyl groups directly bound to zinc are known to form stable zinc bridges between zinc atoms. Thus, lower dialkylzinc compounds are volatile nonpolar liquids while dialkynylzinc species are solids and have very low solubilities in nonpolar organic solvents. In this context, diarylzinc compounds are a middle ground case: while

(20) Concentration of starting materials: aldehyde (0.25 M), Et₂Zn (0.33 M), and Ph₂Zn (0.16 M).

(21) Concentration of ethylphenylzinc was estimated to be 0.32 M, based on the assumption that the equilibrium is completely shifted toward the formation of the mixed zinc species.

(22) (a) Ashby, E. C.; Laemmle, J.; Neumann, H. M. *Acc. Chem. Res.* **1974**, *7*, 272–280. (b) Ashby, E. C.; Laemmle, J.; Neumann, H. M. *J. Am. Chem. Soc.* **1972**, *94*, 4.

(23) Concentration of starting materials: Aldehyde (0.25 M) and Ph₂Zn (0.27 M).

(24) Oki, M. *Tetrahedron Lett.* **1967**, *8*, 1785–1788.

(25) Yajima, K.; Kawashima, H.; Hashimoto, N.; Miyake, Y. *J. Phys. Chem.* **1996**, *100*, 14936–14940.

(26) Addition of Grignard and alkyllithium reagents to aldehydes should provide lower activation parameters than their corresponding ketone analogues due to reduced steric hindrance. For secondary deuterium kinetic isotope effects in the irreversible additions of allyl reagents to benzaldehyde see: (a) Gajewski, J. J.; Bocian, W.; Brichford, N. L.; Henderson, J. L. *J. Org. Chem.* **2002**, *67*, 4236–4240. For kinetic studies on the amino-alcohol catalyzed dialkylzinc addition to aldehydes see: (b) Buono, F.; Walsh, P. J.; Blackmond, D. G. *J. Am. Chem. Soc.* **2002**, *124*, 13652–13653. (c) Blackmond, D. G. *J. Am. Chem. Soc.* **1998**, *120*, 13349–13353.

(27) Knochel, P.; Jones, P. *Organozinc Reagents*; Oxford University Press: Oxford, UK, 1999.

(28) Boersma, J. In *Comprehensive Organometallic Chemistry*; Wilkinson, G.; Stone, F. G. A., Abel, E. W., Eds.; Pergamon Press: Oxford, UK, 1982; Vol. 2, pp 823–862.

(18) During the preparation of this manuscript a theoretical DFT study on the arylation of ethanal using a simplified achiral ligand system was published, see: Rudolph, J.; Rasmussen, T.; Bolm, C.; Norrby, P. O. *Angew. Chem., Int. Ed.* **2003**, *42*, 3002–3005.

(19) For recent applications of in situ FT-IR see: (a) Evans, D. A.; Scheidt, K. A.; Johnston, J. N.; Willis, M. C. *J. Am. Chem. Soc.* **2001**, *123*, 4480–4491. (b) Sun, X.; Kenkre, S. L.; Remenar, J. L.; Gilchrist, J. H.; Collum, D. B. *J. Am. Chem. Soc.* **1997**, *119*, 4765–4766. (c) Kainz, S.; Brinkmann, A.; Leitner, W.; Pfaltz, A. *J. Am. Chem. Soc.* **1999**, *121*, 6421–6429. (d) Marchueta, M.; Olivella, S.; Solà, L.; Moyano, A.; Pericàs, M. A.; Riera, A. *Org. Lett.* **2001**, *3*, 3197–3200.

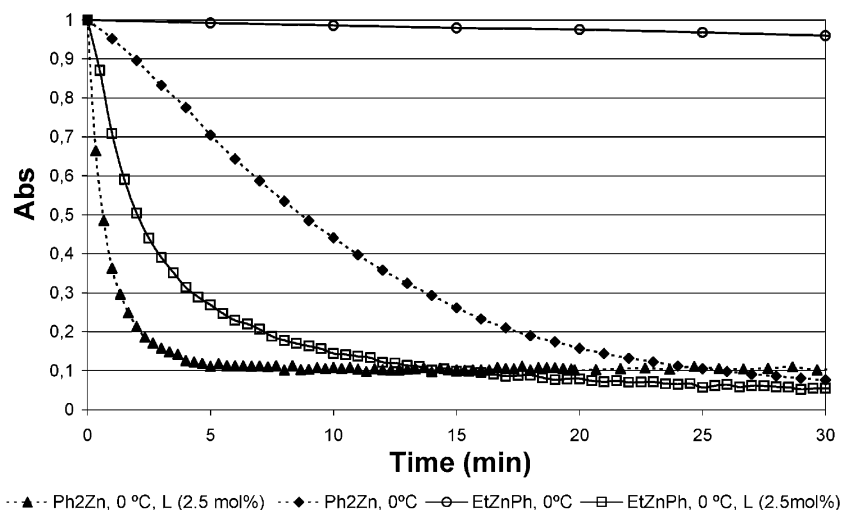


FIGURE 4. Comparison of the catalyzed vs the background process at 0 °C.

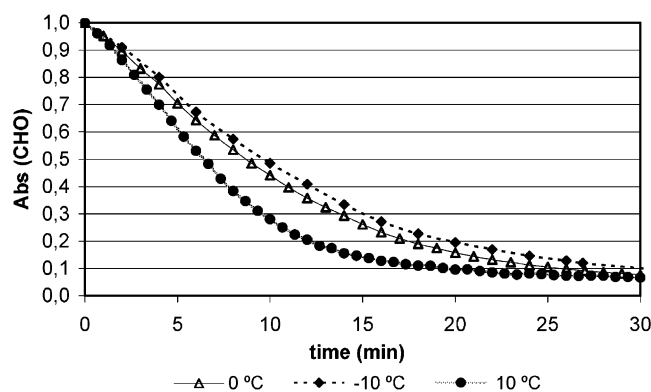


FIGURE 5. Background reaction with Ph_2Zn at different temperatures.

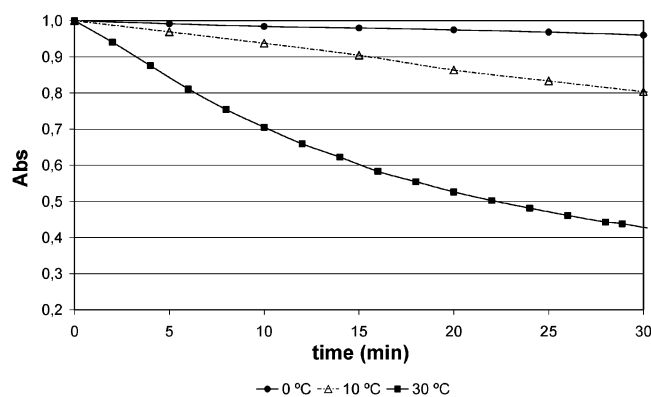


FIGURE 6. Background reaction using the $\text{Et}_2\text{Zn}/\text{Ph}_2\text{Zn}$ mixture at different temperatures.

they are believed to exist in a monomeric form in solution, Ph_2Zn is a solid with a melting point of 107 °C and exhibits a decreased solubility compared to plain dialkylzinc compounds.²⁸ To gain further insight into the mechanism and the nature of the species formed when mixing diphenylzinc and diethylzinc a computational study was undertaken. All calculations were made using density functional theory (DFT) with the B3LYP functional. Geometry and energy optimization were run using a LACVP* basis set that includes Hay and Wadt's

effective core potential (ECP) for zinc, while carbon atoms are described using a 6-31G* basis set.^{29,30}

As a first step we investigated the simple methyl exchange between two molecules of Me_2Zn to determine whether the method results were in agreement with the physical properties of this compound. A four-center symmetric transition state **TS-II** (Figure 7) was localized in which the exchanging methyl groups are 2.27 Å away from each metal center. From this point, geometry and energy optimization led to a loosely bound dimer (**D-I**) 5.93 kcal·mol⁻¹ more stable than **TS-II** and only 1.53 kcal·mol⁻¹ more stable than two monomer molecules. Relative energies for the methyl exchange process (Table 5) predict that alkyl (methyl) exchange is a kinetically feasible process but that aggregation between dialkylzinc species is not thermodynamically favored since entropic factors should prevail over the small stabilizing effects found for **D-I** with respect to monomeric Me_2Zn . This is in agreement with experimental observations of Me_2Zn being a liquid with a low boiling point.

In the case of diphenylzinc, X-ray crystallography studies show this compound exists as a dimer in the solid state as has been demonstrated by Bickelhaupt and co-workers.³¹ The structure of $(\text{Ph}_2\text{Zn})_2$ was modeled at the same theory level to further check whether density functional theory could correctly predict the structure of this class of compounds. The optimized structure for the diphenylzinc dimer (**D-III**) is shown in Figure 7. The main structural features of **D-III** fully coincide with the reported solid-state X-ray structure. The central four-membered ring is nonplanar with a ring folding along the Zn–Zn axis of around 25°. The interactions between the two Ph_2Zn moieties were correctly predicted: the distances Zn–C(aromatic) within the two monomers are 2.44 and 2.36 Å for the crystal structure and 2.51 and 2.52 Å for the calculated model (**D-III**).

For the ethyl–phenyl exchange a four-center transition state could be found (**TS-V**) in which the phenyl group to be transferred is perpendicular to the four-center

(29) *Spartan 02*; Wavefunction, Inc.; Irvine, CA.

(30) Hay, P. J.; Wadt, W. R. *J. Chem. Phys.* **1985**, *82*, 270–283.

(31) Markies, P. R.; Schat, G.; Akkerman, O. S.; Bickelhaupt, F. *Organometallics* **1990**, *9*, 2243–2247.

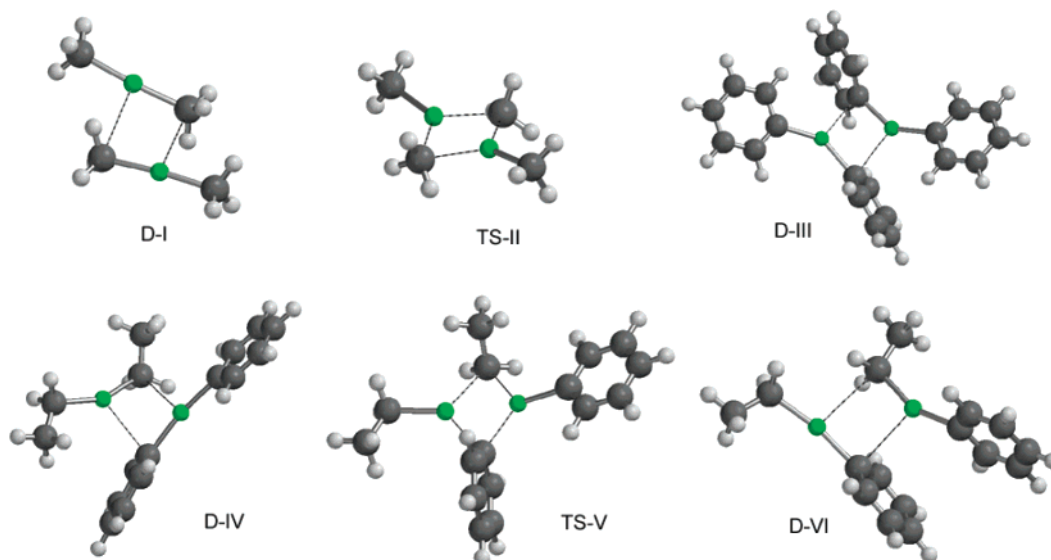


FIGURE 7.

TABLE 5. Computed Absolute and Relative Energies of Species Involved in the Me_2Zn Interchange

compd	absolute ΔH_f (au)	relative ΔH_f (kcal·mol ⁻¹)
$2 \times \text{Me}_2\text{Zn}$	-290.784 516	1.53
D-I	-290.786 966	0.00
TS-II	-290.777 507	5.93

TABLE 6. Computed Absolute and Relative Energies of Species Involved in $\text{Et}_2\text{Zn}/\text{Ph}_2\text{Zn}$ Interchange

compd	absolute ΔH_f (au)	relative ΔH_f (kcal·mol ⁻¹)
$1/2 \text{D-III} + \text{Et}_2\text{Zn}$	-752.872 412	0.00
$\text{Ph}_2\text{Zn} + \text{Et}_2\text{Zn}$	-752.863 229	5.76
D-IV	-752.869 430	1.87
TS-V	-752.867 368	3.16
D-VI	-752.872 111	0.19
$2 \times \text{EtPhZn}$	-752.864 166	5.17

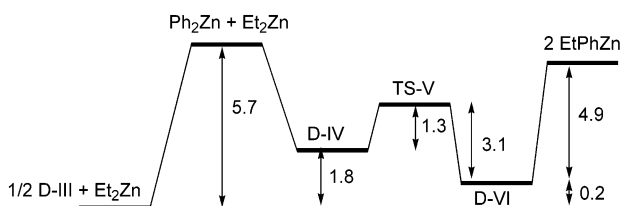


FIGURE 8. Energy profile for the formation of EtPhZn.

reaction core (Figure 7). The aromatic carbon atom directly attached to both metal centers adopts a distorted tetrahedral geometry with a Zn–C–Zn angle of 72°. Most surprisingly, the heat of formation found for **TS-V** is lower than that of either of the starting materials ($\text{Ph}_2\text{Zn} + \text{Et}_2\text{Zn}$) or of the exchanged product ethylphenylzinc (Table 6 and Figure 8). Perturbation and energy optimization from **TS-V** led to the localization of dimers **D-IV** and **D-VI** (Figure 7) with relative energies 1.87 and 0.19 kcal·mol⁻¹, respectively (Table 6). Both **D-IV** and **D-VI** show higher interaction energy than the analogous dimethylzinc aggregate **D-I**, as can be deduced from the shorter Zn–C distances between monomers and bigger distortion from linear geometry (although less than for

the diphenylzinc dimer, **D-III**). Starting from the Et_2Zn and $1/2 \text{D-III}$ the resulting energy profile for the formation of the mixed EtPhZn is depicted in Figure 8.

The most stable species in the reaction profile correspond to the starting materials ($\text{Et}_2\text{Zn} + 1/2 \text{D-III}$) and the symmetrical dimer formed by two molecules of EtPhZn (**D-VI**). On the other hand, the mixtures of discrete ($\text{Et}_2\text{Zn} + \text{Ph}_2\text{Zn}$) and ($2 \times \text{EtPhZn}$) are energetically disfavored by approximately 5.76 and 5.17 kcal·mol⁻¹. Taking into account only the monomeric species, the formation of EtPhZn is moderately favored by only 0.6 kcal·mol⁻¹, while if we consider the formation of aggregates (dimers) the process is slightly disfavored, $\Delta E = 0.19$ kcal·mol⁻¹. From the FT-IR study (vide supra), we can ascertain that when mixing Et_2Zn and Ph_2Zn in a 2:1 ratio, diphenylzinc is not available in high concentrations in the reaction mixture since the rate of the background addition reaction is much slower than when using Ph_2Zn alone. The present theoretical model (Figure 8) indicates that alkyl–aryl interchange between different zinc species is a kinetically facile process since the transition state identified for the Et–Ph exchange **TS-V** represents a low energy barrier. The energies calculated in the gas phase for the different species predict the formation of the mixed zinc species as a basically thermo neutral process. This is not in agreement with the experimental observations that point to an equilibrium predominantly shifted toward the formation of EtPhZn. Still, entropy and solvation factors which are not evaluated in the present study could account for the preferential formation of EtPhZn. Diphenylzinc has been calculated to be monomeric in hexane at concentrations of 0.001–0.005 M, and its solubility has been calculated to be 0.015 M in the same solvent.³¹ In the present arylation reactions and in the FT-IR studies Ph_2Zn was used at much higher concentration (0.15–0.25 M) in toluene. The experimental facts along with the calculated model may suggest that mixing Et_2Zn and Ph_2Zn (2/1) at a concentration between 0.15 and 0.25 M leads to the

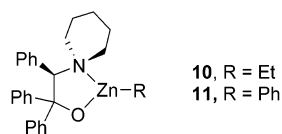
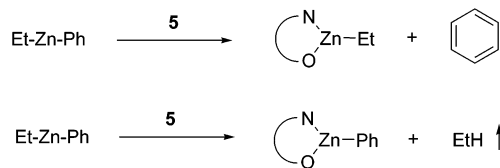


FIGURE 9.

SCHEME 2



formation of EtPhZn, which in turn can exist in equilibrium between its monomer and its dimer or a higher aggregate.

Two arguments are in favor of the phenyl group being transferred to the aldehyde from a mixed species. On one hand, the comparison of the experimentally determined activation energies for the noncatalytic transfer of phenyl from Ph_2Zn and EtPhZn, along with the DFT-calculated activation energy for the Ph/Et scrambling, suggest that, under the Curtin–Hammett principle, if Ph_2Zn were present at all in the reaction medium it would lead to the rapid arylation from Ph_2Zn , which is not the case. On the other hand, the complete transfer of the phenyl groups when using a substoichiometric amount of diphenylzinc can only be explained if transfer is taking place from a mixed species arising from group exchange between Et_2Zn and Ph_2Zn . In addition, differential calorimetric studies performed by Nehl et al. on binary mixtures of diorganozinc compounds are consistent with an equilibrium completely shifted toward the mixed species when using Ph_2Zn .³²

Experimental Studies on the Nature of the Catalytic Species. The active species in the β -amino-alcohol catalyzed asymmetric dialkylzinc addition to aldehydes is a five-member-ring chelate in which the Zn atom is attached to both nitrogen and oxygen and to an alkyl group (Figure 9). If only diethylzinc is used, the R group on Zn will be ethyl (**10**), and when only Ph_2Zn is used a Zn–Ph moiety should be part of the active catalyst (**11**). When using a $\text{Ph}_2\text{Zn}/\text{Et}_2\text{Zn}$ mixture a more complex situation arises and, in principle, either Zn–Et or Zn–Ph moieties could form and serve as active catalytic species. To respond to this question a simple experiment was envisaged. Diethylzinc (0.64 mmol) and diphenylzinc (0.64 mmol) were mixed together in toluene and allowed to equilibrate for 15–30 min to allow for the formation of the mixed EtPhZn. To this mixture the amino alcohol **5** (1.0 mmol) was added in one portion and the volume of generated gas was measured. If **10** were formed exclusively an equal amount of benzene would be produced, while if the alkyl group on Zn were phenyl (**11**) the evolution of 1.0 mmol of ethane should be observed (Scheme 2). The gas evolution was measured with a gas buret. Upon carrying out the experiment, 2 mL (0.09 mmol) of ethane was collected out of a theoretical maximum of 22.4 mL (1.0 mmol).³³ This result indicates that the phenyl groups on zinc react faster than the alkyl

(32) Nehl, H.; Scheidt, W. R. *J. Organomet. Chem.* **1985**, *289*, 1–8.

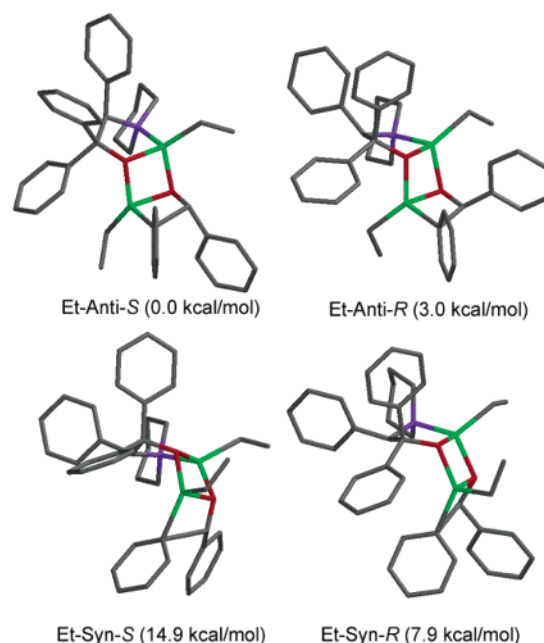


FIGURE 10. PM3(tm) tricyclic transition states for catalyst **10**.

ones with the hydroxyl groups of the ligand, and that the active catalytic complex when using the $\text{Et}_2\text{Zn}/\text{Ph}_2\text{Zn}$ mixture is predominantly **10**.³⁴

Computational Study on the Enantioselective Phenyl Transfer. On the basis of the preceding results the asymmetric phenyl transfer from monomeric EtPhZn catalyzed by **10** and **11** was modeled. The large size of the transition state structures involved and computational time restrictions enforced the use of a semiempirical PM3(tm) method. Transition state structures calculated at the PM3 level reproduce the results of much more time-consuming methods (DFT, MP2) and are able to predict the sense of enantioselection in most cases.^{8c,35} Thus the stereochemical outcome of the reaction was studied considering the four diastereomeric transition state structures (*anti*-(*S*), *syn*-(*S*), *anti*-(*R*), *syn*-(*R*)) which, according to the seminal work of Noyori, should determine the final selectivity.³⁶ Conformational isomerism coming from the rotation of the nontransferred ethyl groups and the five-membered-ring chelate with the ligand was thoroughly studied. The four most stable TS structures located for each catalytic species **10** and **11** are depicted in Figures 10 and 11 along with their corresponding relative energies. Vibration analysis revealed imaginary stretching frequencies of 339i (Et-Anti-

(33) In a similar experiment, a pre-equilibrated mixture of Et_2Zn (1 mmol) and Ph_2Zn (0.5 mmol) was treated with 1.5 mmol of **5**. Upon addition of the amino alcohol 11 mL of ethane was collected, which corresponds to 0.5 mmol of Et_2Zn in excess, out of a maximum of 33 mL.

(34) The present experiment suggests that formation of **10** is kinetically favored over **11**. However, during the course of the reaction scrambling between ethyl and phenyl on the Zn center of the catalyst cannot be ruled out.

(35) (a) Kozłowski, M. A.; Dixon, S. L.; Panda, M.; Lauri, G. *J. Am. Chem. Soc.* **2003**, *125*, 6614–6615. (b) Panda, M.; Phuan, P.-W.; Kozłowski, M. C. *J. Org. Chem.* **2003**, *68*, 564–571. (c) Goldfuss, B.; Steigelmann, M.; Khan, S. I.; Houk, K. N. *J. Org. Chem.* **2000**, *65*, 77–82. (d) Vazquez, J.; Pericás, M. A.; Maseras, F.; Lledos, A. *J. Org. Chem.* **2000**, *65*, 7303–7309.

(36) Yamakawa, M.; Noyori, R. *Organometallics* **1999**, *18*, 128–133.

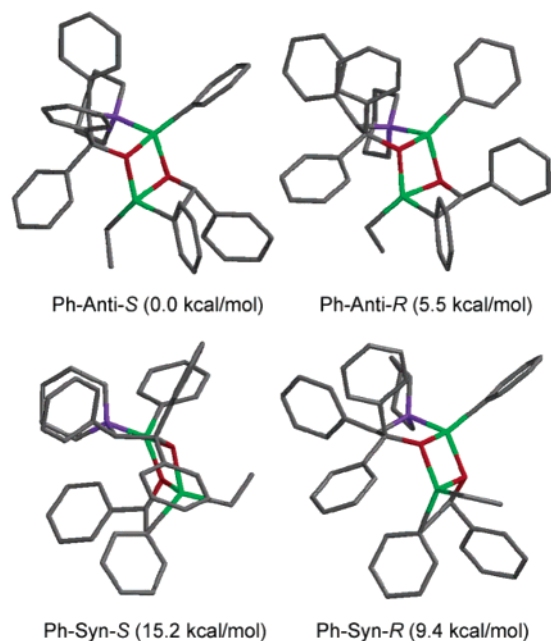


FIGURE 11. PM3(tm) tricyclic transition states for catalyst **11**.

S) and $336i\text{ cm}^{-1}$ (Ph-Anti-*S*) for the forming C–C bond between the transferred aryl and the aldehyde. As occurs in the ethylation process, there exists a considerable energy gap between syn and anti TS structures, the latter ones being more favored. In this context, reaction selectivity should be determined exclusively on the basis of Anti-*S* and Anti-*R* energy variations. To our delight, the stereochemical course of the arylation reaction was correctly predicted by the present model. Thus, when employing (*R*)-2-piperidino-1,1,2-triphenylethanol **5**, Anti-*S*, the most stable TS structure would lead to the experimentally observed (*S*) diarylcarbinols. This trend was observed for both catalytic species **10** and **11**. The energy difference between TS structures, Et-Anti-*S* – Et-Anti-*R* ($3.0\text{ kcal}\cdot\text{mol}^{-1}$) and Ph-Anti-*S* – Ph-Anti-*R* ($5.5\text{ kcal}\cdot\text{mol}^{-1}$), is in agreement with the experimentally observed enantioselectivity. Most interestingly, on the basis of this model, the catalyst containing a Ph–Zn moiety **11** should, in principle, be more selective than **10**. Experimentally, when performing the arylation exclusively with Ph_2Zn a notable selectivity is observed (88% ee, Table 2, entry 6), although this is still lower than that obtained when using the $\text{Et}_2\text{Zn}/\text{Ph}_2\text{Zn}$ mixture. We believe that under these circumstances two different trends coexist: an enhanced selectivity for aryl transfer due to higher selectivity of catalyst **11** and a deleterious uncatalyzed reaction that lowers the product enantiomeric excess. Thus, when using the $\text{Et}_2\text{Zn}/\text{Ph}_2\text{Zn}$ mixture, the benefits of shutting down the uncatalyzed process pay off the use of a slightly less selective catalyst (**10**). The present theoretical study shows that the amino alcohol-catalyzed asymmetric aryl transfer can be conveniently modeled at the PM3(tm) level by means of the energy evaluation of anti and syn 5/4/4 tricyclic TS structures. Moreover, the model of **10** and **11** as active catalysts and EtPhZn as a phenyl source can correctly predict the sense and the selectivity of the overall process.

Conclusions

In summary, the present studies provide a precise picture of the different aspects controlling the stereochemical outcome of the catalytic phenylation of aldehydes: The importance of background, noncatalytic additions for the most usual reacting systems has been assessed, and the reasons for the superior performance of $\text{Ph}_2\text{Zn}/\text{Et}_2\text{Zn}$ as the phenylation reagent thus have been demonstrated. We have provided experimental evidence in favor of the EtPhZn as the largely predominating phenyl delivering species when mixtures of Ph_2Zn and Et_2Zn of the usual composition (1:2) are employed, and have also provided experimental evidence on the nature of the active catalytic species when an amino alcohol ligand is combined with this mixed diorganozinc reagent.

The nature of the equilibria involved in the formation of the mixed diorganozinc species and the importance of the energy barriers associated with their establishment have been addressed by theoretical methods with DFT theory.

All together, the kinetic, experimental, and theoretical studies reported here provide a comprehensive picture of the different aspects involved in the most synthetically useful phenylation reaction.

From a more practical perspective, we have identified a readily available, yet extremely active ligand for the highly enantioselective phenylation of aromatic aldehydes showing promise for large-scale application and have shown its suitability for a full range of substrates. The enantioselectivity recorded with this ligand has been rationalized through a theoretical PM3(tm) study of the nature of the diastereomeric transition states involved in the phenylation of benzaldehyde when 2-piperidino-1,1,2-triphenylethanol is used as ligand in combination with EtPhZn .

Application of this catalytic system to the phenylation of other unsaturated systems is underway in our laboratories.

Experimental Section.

Arylation Reactions under High Dilution Conditions: Typical Experimental Procedure. To a Schlenk flask under nitrogen were added solvent (25 mL), (*R*)-2-piperidino-1,1,2-triphenylethanol (36 mg, 0.1 mmol), and diethylzinc 1 M in hexane (0.025 mL, 0.025 mmol). The reaction mixture was stirred at room temperature for 15 min and then transferred via cannula to Ph_2Zn (55 mg, 0.25 mmol). Stirring was continued for 20 min and then the aldehyde (0.25 mmol) was added. The reaction mixture was stirred at room temperature for 24 h and quenched with HCl (1 M, 15 mL). The aqueous layer was extracted with hexane and the organic layers were combined and dried with $\text{Mg}(\text{SO}_4)_2$. Evaporation of the solvent in vacuo and purification by flash chromatography (SiO_2 , hexane, and hexane/ethyl acetate 98:2) gave the secondary alcohol. Enantiomeric excess was determined by HPLC.

Arylation Reactions Using a Mixture of $\text{Et}_2\text{Zn}/\text{Ph}_2\text{Zn}$: Typical Experimental Procedure. Diphenylzinc (70 mg, 0.32 mmol) was charged into a Schlenk flask in a drybox. The flask was removed from the drybox and freshly distilled solvent (6 mL) was added followed by Et_2Zn 1 M in hexane (0.66 mL, 0.66 mmol). The reaction mixture was stirred for 20 min at room temperature and then (*R*)-2-piperidino-1,1,2-triphenylethanol (18 mg, 0.05 mmol) was added. The resulting solution

was stirred for 20 min and then cooled to the desired temperature. Next, the aldehyde (0.5 mmol) was added and the reaction mixture was monitored by TLC. The reaction was quenched by adding NH_4Cl solution (10 mL) and was extracted with CH_2Cl_2 (3×10 mL). The organic layers were combined and dried over MgSO_4 and the solvent was evaporated in vacuo. Flash chromatography of the crude product (SiO_2 , hexane, and hexane/ethyl acetate 98:2) afforded the pure secondary alcohol. Enantiomeric excess was determined by chiral HPLC.

Arylation Reactions Using 1.5 mol % of Catalyst. The reactions were conducted using a Cooled Carousel Reaction Station under argon atmosphere. To a solution of diphenylzinc (586 mg, 2.67 mmol) in toluene (50 mL) was added diethylzinc 1 M in hexane (5.40 mL, 5.40 mmol) at room temperature. The reaction was stirred at this temperature for 20 min and then 22 mg of (*R*)-2-piperidino-1,1,2-trifluorethanol (0.062 mmol) was added. After the mixture had been stirred for 20 min, 6.6 mL of the solution was transferred to each carousel tube and the station was cooled to 10 °C by means of an immersion cooler with a flexible cooling coil. The aldehyde was added (0.5 mmol) and the resulting reaction was allowed to proceed for 4 h. The reactions were quenched by addition of NH_4Cl solution (10 mL) and were extracted with CH_2Cl_2 (3×10 mL). The organic layers were combined and dried with $\text{Mg}(\text{SO}_4)_2$. Evaporation of the solvent under reduced pressure and purification by column chromatography (SiO_2 , hexane, and hexane/AcOEt 98:2) gave the desired secondary alcohol. Enantiomeric excess was determined by chiral HPLC.

(S)-(4-Tolyl)phenylmethanol.^{6a} R_f (silica gel, hexane/AcOEt, 3:1): 0.50. ^1H NMR (400 MHz, CDCl_3): δ 1.26 (s, 1H), 2.32 (s, 3H), 5.79 (s, 1H), 7.13 (d, $J = 8$ Hz, 2H), 7.24–7.37 (m, 7H) ppm. ^{13}C NMR (100 MHz, CDCl_3): δ 21.2, 76.2, 126.6, 126.7, 127.6, 128.6, 129.3, 137.4, 141.1, 144.1 ppm. MS (EI) m/e : 197 (M – H⁺), 183 (M – CH₃), 121 (M – C₆H₅), 91 (C₇H₇⁺), 77 (C₆H₅⁺). HPLC: Daicel CHIRALCEL-OD. Hexane/*i*-PrOH 90:10, 0.5 mL/min, $\lambda = 254$ nm, $t_R(S) = 19.1$ min, $t_R(R) = 21.1$ min.

(S)-(2-Naphthyl)phenylmethanol.^{6a} R_f (silica gel, hexane/AcOEt, 3:1): 0.47. IR (KBr): ν_{max} 3349 (broad), 3051, 1600, 1492 cm^{-1} . ^1H NMR (400 MHz, CDCl_3): δ 2.34 (s, 1H), 5.99 (s, 1H), 7.24–7.35 (m, 3H), 7.40–7.47 (m, 5H), 7.77–7.83 (m, 3H), 7.88 (s, 1H) ppm. ^{13}C NMR (100 MHz, CDCl_3): δ 76.4, 124.7, 125.0, 125.9, 126.2, 126.7, 127.7, 128.1, 128.3, 128.5, 132.9, 133.3, 141.1, 143.6 ppm. HPLC: Daicel CHIRALCEL-OD. Hexane/*i*-PrOH 90:10, 1.0 mL/min, $\lambda = 254$ nm, $t_R(S) = 16.0$ min, $t_R(R) = 21.1$ min.

(S)-(4-Methoxyphenyl)phenylmethanol.^{6a} R_f (silica gel, hexane/AcOEt, 3:1): 0.31. IR (KBr): ν_{max} 3350 (broad), 3050, 1613, 1514 cm^{-1} . ^1H NMR (400 MHz, CDCl_3): δ 2.18 (s, 1H), 3.78 (s, 3H), 5.80 (s, 1H), 6.88–6.85 (m, 3H), 7.24–7.38 (m, 6H) ppm. HPLC: Daicel CHIRALCEL-OD. Hexane/*i*-PrOH 95:5, 1.0 mL/min, $\lambda = 254$ nm, $t_R(S) = 23.9$ min, $t_R(R) = 22.7$ min.

(R)-1-Phenylheptanol.^{6b} R_f (silica gel, hexane/AcOEt, 3:1): 0.53. ^1H NMR (400 MHz, CDCl_3): δ 0.86 (t, $J = 6.8$ Hz, 3H), 1.21–1.43 (m, 8H), 1.64–1.83 (m, 2H), 1.97 (s broad, 1H), 4.63 (t, $J = 6.6$ Hz, 1H), 7.24–7.28 (m, 1H), 7.31–7.33 (m, 4H) ppm. ^{13}C NMR (100 MHz, CDCl_3): δ 14.3, 22.8, 26.0, 29.4, 32.0, 39.3, 74.9, 126.1, 127.7, 128.6, 145.2 ppm. HPLC: Daicel CHIRALCEL-OD. Hexane/*i*-PrOH 95:5, 0.5 mL/min, $\lambda = 254$ nm, $t_R(S) = 15.5$ min, $t_R(R) = 14.6$ min.

(S)-(4-Chlorophenyl)phenylmethanol.^{6b} R_f (silica gel, hexane/AcOEt, 3:1): 0.48. IR (KBr): ν_{max} 3260 (broad), 3050, 1600, 1493, cm^{-1} . ^1H NMR (300 MHz, CDCl_3): δ 1.26 (s, 1H), 5.81 (s, 1H), 7.25–7.35 (m, 9H) ppm. ^{13}C NMR (75 MHz, CDCl_3): δ 75.6, 126.5, 127.9, 128.6, 128.6, 128.7, 133.3, 142.2, 143.5 ppm. HPLC: acetate derivative: Daicel CHIRALCEL-OD. Hexane/*i*-PrOH 99:1, 0.2 mL/min, $\lambda = 254$ nm, $t_R(S) = 37.9$ min, $t_R(R) = 39.6$ min. HPLC: *p*-nitrobenzoate derivative: Daicel CHIRALCEL-OD. Hexane/*i*-PrOH 98:2, 0.5 mL/min, $\lambda = 254$ nm, $t_R(S) = 44.1$ min, $t_R(R) = 40.5$ min.

(S)-(3-Tolyl)phenylmethanol.³⁷ $[\alpha]_D -12.5$ (c 0.60, CHCl_3). R_f (silica gel, hexane/AcOEt, 3:1): 0.54. ^1H NMR (400 MHz, CDCl_3): δ 2.17 (d, $J = 3.6$ Hz, 1H), 2.33 (s, 3H), 5.81 (d, $J = 3.6$ Hz, 1H), 7.07–7.28 (m, 5H), 7.31–7.40 (m, 4H) ppm. ^{13}C NMR (100 MHz, CDCl_3): δ 21.7, 76.5, 123.8, 126.7, 127.4, 127.7, 128.5, 128.6, 128.7, 138.4, 144.0, 144.1 ppm. ^{19}F NMR (376 MHz, CDCl_3) Mosher ester derivative: -73.84 , -73.96 (major) ppm.

(S)-(2-Tolyl)phenylmethanol.³⁸ R_f (silica gel, hexane/AcOEt, 3:1): 0.53. IR (KBr): ν_{max} 3240 (broad), 3075, 1603, 1491 cm^{-1} . ^1H NMR (400 MHz, CDCl_3): δ 2.21 (s, 3H), 2.28 (s, 1H), 5.94 (s, 1H), 7.10–7.30 (m, 8H), 7.47–7.49 (m, 1H) ppm. ^{13}C NMR (100 MHz, CDCl_3): δ 19.5, 73.4, 126.2, 126.4, 127.2, 127.6, 127.7, 128.6, 130.6, 135.5, 141.5, 142.9 ppm. HPLC: Daicel CHIRALCEL-OD. Hexane/*i*-PrOH 99:1, 1.0 mL/min, $\lambda = 254$ nm, $t_R(S) = 64.2$ min, $t_R = 58.2$ min. HPLC: Daicel CHIRALPACK-AD. Hexane/*i*-PrOH 98:2, 0.5 mL/min, $\lambda = 254$ nm, $t_R(S) = 36.48$ min, $t_R(R) = 38.55$ min.

(S)-(2-Chlorophenyl)phenylmethanol.³⁹ R_f (silica gel, hexane/AcOEt, 3:1): 0.43. ^1H NMR (400 MHz, CDCl_3): δ 2.58 (s broad, 1H), 6.17 (s, 1H), 7.16–7.37 (m, 8H), 7.56–7.58 (m, 1H) ppm. ^{13}C NMR (100 MHz, CDCl_3): δ 72.7, 127.0, 127.2, 127.8, 128.1, 128.6, 128.8, 129.6, 132.6, 141.1, 142.3 ppm. HPLC: Daicel CHIRALCEL-OD. Hexane/*i*-PrOH 90:10, 0.5 mL/min, $\lambda = 254$ nm, $t_R(S) = 19.8$ min, $t_R(R) = 15.9$ min.

(S)-(2-Fluorophenyl)phenylmethanol.⁴⁰ R_f (silica gel, hexane/AcOEt, 3:1): 0.50. ^1H NMR (400 MHz, CDCl_3): δ 2.47 (s, 1H), 6.14 (s, 1H), 6.99–7.00 (m, 1H), 7.13–7.17 (m, 1H), 7.23–7.36 (m, 4H), 7.39–7.41 (m, 2H), 7.48–7.53 (m, 1H) ppm. ^{13}C NMR (100 MHz, CDCl_3): δ 70.2 (d, $J_{\text{CF}} = 3$ Hz), 115.5 (d, $J_{\text{CF}} = 21.4$ Hz), 124.4 (d, $J_{\text{CF}} = 3.1$ Hz), 126.5, 127.7, 127.8, 127.9, 128.6, 129.2 (d, $J_{\text{CF}} = 8.4$ Hz), 131.1 (d, $J_{\text{CF}} = 13$ Hz), 160.0 (d, $J_{\text{CF}} = 244.6$ Hz) ppm. ^{19}F NMR (376 MHz, CDCl_3): 118.84 ppm. HPLC: Daicel CHIRALCEL-OD. Hexane/*i*-PrOH 95:5, 0.5 mL/min, $\lambda = 270$ nm, $t_R(S) = 26.5$ min, $t_R(R) = 23.1$ min.

(S)-(4-Biphenyl)phenylmethanol.^{6a} R_f (silica gel, hexane/AcOEt, 3:1): 0.42. ^1H NMR (400 MHz, CDCl_3): δ 2.30 (s, 1H), 5.87 (s, 1H), 7.23–7.37 (m, 4H), 7.40–7.45 (m, 6H), 7.54–7.57 (m, 4H) ppm. ^{13}C NMR (100 MHz, CDCl_3): δ 76.2, 126.7, 127.1, 127.2, 127.4, 127.5, 127.8, 128.7, 128.9, 140.6, 140.9, 143.0, 143.9 ppm. HPLC: Daicel CHIRALCEL-OD. Hexane/*i*-PrOH 94:6, 0.8 mL/min, $\lambda = 254$ nm, $t_R(S) = 32.4$ min, $t_R(R) = 29.8$ min.

(R)-(E)-1,3-Diphenyl-2-propenol.^{6b} R_f (silica gel, hexane/AcOEt, 3:1): 0.50. ^1H NMR (400 MHz, CDCl_3): δ 2.35 (s broad, 1H), 5.34 (d, $J = 7$ Hz, 1H), 6.37 (dd, $J = 7$ Hz, $J = 16$ Hz, 1H), 6.65 (d, $J = 16$ Hz, 1H), 7.23–7.37 (m, 4H), 7.19–7.42 (m, 6H) ppm. ^{13}C NMR (100 MHz, CDCl_3): δ 75.4, 126.6, 126.9, 127.4, 128.0, 128.8, 128.9, 130.8, 131.8, 136.8, 143.1 ppm. HPLC: Daicel CHIRALCEL-OD. Hexane/*i*-PrOH 90:10, 1.0 mL/min, $\lambda = 254$ nm, $t_R(S) = 15.9$ min, $t_R(R) = 20.4$ min.

(R)-(E)-2-Methyl-1,3-diphenyl-2-propenol.⁴¹ $[\alpha]_D -4.85$ (c 1.6/ CHCl_3). R_f (silica gel, hexane/AcOEt, 3:1): 0.47. ^1H NMR (400 MHz, CDCl_3): δ 1.73 (d, $J = 1.2$ Hz, 3H), 2.11 (s broad, 1H), 5.27 (s, 1H), 6.77 (s broad, 1H), 7.21–7.23 (m, 1H), 7.28–7.37 (m, 7H), 7.42–7.44 (m, 2H) ppm. ^{13}C NMR (100 MHz, CDCl_3): δ 14.3, 79.7, 126.3, 126.7, 126.8, 127.8, 128.4, 128.7, 129.3, 137.7, 139.8, 142.3 ppm. HPLC: *p*-nitrobenzoate derivative: Daicel CHIRALCEL-OD. Hexane/*i*-PrOH 95:5, 0.5 mL/min, $\lambda = 254$ nm, $t_R(S) = 26.9$ min, $t_R(R) = 29.8$ min.

(R)-2-Ethyl-1-phenylbutanol.⁴² $[\alpha]_D -8.08$ (c 0.26, CHCl_3). R_f (silica gel, hexane/AcOEt, 3:1): 0.66. IR (KBr): ν_{max} 3417

(37) Guijarro, D.; Yus, M. *Tetrahedron* **2000**, *56*, 1135–1138.

(38) Huang, W.-S.; Pu, L. *Tetrahedron Lett.* **1999**, *41*, 145–149.

(39) Zhao, G.; Li, X. G.; Wang, X. R. *Tetrahedron: Asymmetry* **2001**, *12*, 399–403.

(40) Ohkuma, T.; Koizumi, M.; Ikehira, H.; Yokozawa, T.; Noyori, R. *Org. Lett.* **2000**, *2*, 659–662.

(41) Nudelman, N. S.; Garcia, G. V. *J. Org. Chem.* **2001**, *66*, 1387–94.

(42) Calas, M.; Calas, B.; Giral, L. *Bull. Soc. Chim. Fr.* **1973**, 2079–2086.

(broad), 3050, 2964, 1451, 1017 cm^{-1} . ^1H NMR (400 MHz, CDCl_3): δ 0.85 (t, $J = 7$ Hz, 3H), 0.90 (t, $J = 7$ Hz, 3H), 1.15–1.23 (m, 1H), 1.24–1.33 (m, 2H), 1.40–1.61 (m, 2H), 1.75 (broad s, 1H), 4.64 (d, $J = 6.4$ Hz, 1H), 7.25–7.28 (m, 1H), 7.31–7.34 (m, 4H) ppm. ^{13}C NMR (100 MHz, CDCl_3): δ 11.1, 11.5, 20.8, 22.0, 48.0, 76.1, 126.7, 127.5, 128.5, 144.3 ppm. HPLC: Daicel CHIRALCEL-OD. Hexane/*i*-PrOH 93:7, 0.5 mL/min, $\lambda = 254$ nm, $t_{\text{R}}(\text{S}) = 11.1$ min, $t_{\text{R}}(\text{R}) = 16.4$ min.

(R)-Cyclohexylphenylmethanol.⁴³ $[\alpha]_{\text{D}} +17.0$ (*c* 0.60, CHCl_3). R_{f} (silica gel, hexane/AcOEt, 3:1): 0.61. ^1H NMR (400 MHz, CDCl_3): δ 0.88–1.28 (m, 5H), 1.36–1.39 (m, 1H), 1.56–1.68 (m, 3H), 1.75–1.81 (m, 2H), 1.97–2.00 (m, 1H), 4.36 (d, $J = 7$ Hz, 1H), 7.25–7.36 (m, 5H) ppm. ^{13}C NMR (100 MHz, CDCl_3): δ 26.2, 26.3, 26.6, 29.0, 29.5, 45.2, 79.6, 126.8, 127.6, 128.4, 143.8 ppm. HPLC: Daicel CHIRALCEL-OD. Hexane/*i*-PrOH 95:5, 0.5 mL/min, $\lambda = 254$ nm, $t_{\text{R}}(\text{S}) = 14.8$ min, $t_{\text{R}}(\text{R}) = 18.0$ min.

(R)-2,2-Dimethyl-1-phenylpropanol.^{6c} R_{f} (silica gel, hexane/AcOEt, 3:1): 0.62. IR (KBr): ν_{max} 3424 (broad), 3050, 2954, 1451, 1385 cm^{-1} . ^1H NMR (400 MHz, CDCl_3): δ 0.92 (s, 9H), 1.85 (s, 1H), 4.40 (s, 1H), 7.24–7.32 (m, 5H) ppm. ^{13}C NMR (100 MHz, CDCl_3): δ 26.1, 35.8, 82.6, 127.4, 127.7, 127.8, 142.3 ppm. HPLC: Daicel CHIRALCEL-OD. Hexane/*i*-PrOH 98:2,

0.5 mL/min, $\lambda = 254$ nm, $t_{\text{S}} = 20.4$ min, $t_{\text{R}} = 31.4$ min. GC: β -DEX 120 Column, 120 $^{\circ}\text{C}$: $t_{\text{R}}(\text{S}) = 44.3$ min, $t_{\text{R}}(\text{R}) = 45.5$ min.

(S)-(3-Methoxyphenyl)phenylmethanol.^{6a} R_{f} (silica gel, hexane/AcOEt, 3:1): 0.33. ^1H NMR (400 MHz, CDCl_3): δ 2.40 (broad s, 1H), 3.75 (s, 3H), 5.76 (s, 1H), 6.77–6.80 (m, 1H), 6.91–6.93 (m, 2H), 7.20–7.36 (m, 6H) ppm. ^{13}C NMR (100 MHz, CDCl_3): δ 55.3, 76.2, 112.2, 113.1, 119.0, 126.6, 127.7, 128.6, 129.6, 143.8, 145.6, 159.8 ppm. HPLC: Daicel CHIRALCEL-OD. Hexane/*i*-PrOH 95:5, 1.0 mL/min, $\lambda = 254$ nm, $t_{\text{R}}(\text{S}) = 27.1$ min, $t_{\text{R}}(\text{R}) = 42.0$ min.

Acknowledgment. We gratefully thank DGI-MCYT (BQU2002-02459) and DURSI (2001SGR50) for financial support. X.V. thanks the MCYT for a Ramón y Cajal research position. We thank Dr. Alex Comely for reading the manuscript. We also thank Mr. Daniel Font for his assistance with the in situ FT-IR experiments.

Supporting Information Available: General experimental methods and Cartesian coordinates and energies for molecular modeling compounds and transition states. This material is available free of charge via the Internet at <http://pubs.acs.org>.

JO0358240

(43) Langer, F.; Schwink, L.; Devasagayaram, A.; Chavant, P.-Y.; Knochel, P. *J. Org. Chem.* **1996**, *61*, 8229–8243.